ELSEVIER

Journal of Nuclear Materials 253 (1998) 213–218

journal of nuclear materials

Density dependence on thermal properties of Li_2TiO_3 pellets

Shigeru Saito [a], Kunihiko Tsuchiya [a,*], Hiroshi Kawamura [a], Takayuki Terai [b], Satoru Tanaka [b]

[a] *Oarai Research Establishment, JAERI, Oarai-machi, Higashi-Ibaraki-gun, Ibaraki-ken 311-13, Japan*
[b] *University of Tokyo, Hongo, Bunkyo-ku, Tokyo 113, Japan*

Abstract

Lithium ceramics have been considered as tritium breeders for fusion reactors. As a part of the study program for fusion blanket development, the characteristics of tritium breeders are estimated for the material selection and fusion blanket design. Among the candidate tritium breeders, lithium titanate (Li_2TiO_3) is regarded as one of the best materials because of many advantages, reasonable lithium atom density, low activation, excellent tritium release characteristic at low temperature, compatibility with structural materials, reprocessing, etc. However, only limited data on the thermal and mechanical characteristics of Li_2TiO_3 have been obtained for breeder material selection and fusion blanket design. In this study, Li_2TiO_3 pellets with three different densities, i.e., 73%T.D., 83%T.D. and 93%T.D., were prepared. Then, the density dependence and the thermal hysteresis of their thermal conductivity, specific heat and thermal expansion were investigated.

1. Introduction

Lithium ceramics have received considerable attention as tritium breeders for fusion reactors [1,2]. Candidate ceramic breeder materials considered at present include Li_2O [3], $LiAlO_2$ [4], Li_2ZrO_3 [5], Li_2TiO_3 [6] and Li_4SiO_4 [7]. Li_2O is attractive for obtaining a suitable tritium breeding ratio (TBR) [8]. $LiAlO_2$, Li_2ZrO_3 and Li_4SiO_4 are attractive because of their better thermochemical stability and reliability in terms of lithium mass transfer and compatibility with other blanket materials, such as the neutron multiplier and structural materials [9].

Recently, lithium titanate (Li_2TiO_3) was proposed as a candidate material in a breeder blanket because tritium is able to be recovered at low temperature [10]. Although it has not been decided yet which is the best breeder material among them, lithium is an important and limited resource. In this sense, reprocessing technology development for ceramic breeders has been proposed to recover lithium for effective resource use, and to remove radioactive isotopes [11]. Li_2TiO_3 is an especially good material from the viewpoint of reprocessing because lithium in Li_2TiO_3 can be selectively dissolved in low HNO_3 concentration [12].

As a part of the study program for fusion blanket development, the characteristics of tritium breeders have been estimated for the material selection and fusion blanket design. However, not enough data on the characteristics of Li_2TiO_3, like thermal properties, mechanical properties, etc., have been obtained for breeder material selection and fusion blanket design.

In this study, three kinds of Li_2TiO_3 pellets with different densities, i.e., 73%T.D., 83%T.D. and 93%T.D., were prepared. Then, density dependence and thermal hysteresis, with respect to thermal conductivity, specific heat and thermal expansion, were investigated.

2. Experimental

2.1. Preparation of Li_2TiO_3

Three kinds of Li_2TiO_3 pellets were prepared from Li_2TiO_3 powder (Soekawa Chemical) The purity and the particle size of Li_2TiO_3 powder were 99.9% and -60 mesh, respectively. The main impurities (in ppm) of Li_2TiO_3 powder were as follows: Na, 16; Al, 17; Ca, 2;

* Corresponding author. Tel.: +81-29 264 8369; fax: +81-29 264 8480; e-mail: tsuchiya@jmtr.oarai.jaeri.go.jp.

0022-3115/98/$19.00
PII S0022-3115(97)00314-0

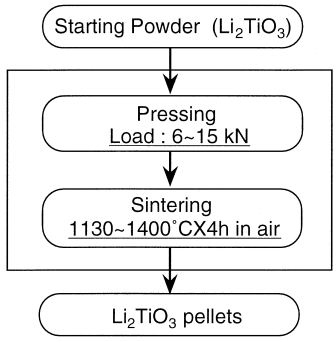

Fig. 1. Flow chart on preparation of three kinds of Li_2TiO_3 pellets.

Zr, <5; Mg, <5; Co, <0.5; Si, 41. A flow chart on preparation of Li_2TiO_3 pellets is shown in Fig. 1. The preparation steps of Li_2TiO_3 pellets are as follows:

1. Li_2TiO_3 powder synthesis
2. cold pressing
3. sintering

Basic properties of Li_2TiO_3 pellets were examined by density measurement and structure observation. The density of the three kinds of Li_2TiO_3 pellets were 73%T.D. (Sample A), 83%T.D. (Sample B) and 93%T.D. (Sample C), respectively. The dimensions of the prepared Li_2TiO_3 pellets were 8 mm diameter by 2 mm thickness.

2.2. Characterization of Li_2TiO_3

Characteristics of the three kinds of Li_2TiO_3 pellets prepared by the different condition were evaluated. As basic properties of the three kinds of Li_2TiO_3 pellets, density, specific surface area, impurities, and chemical phase were measured. The density and the porosity of these pellets were measured by mercury porosimetry. The specific surface area were measured by BET method. Fracture surfaces of each Li_2TiO_3 pellet were examined by scanning electron microscopy (SEM). Impurity levels were measured by atomic emission spectrometry with inductively coupled plasma (ICP-AES) and atomic absorption photometry. Crystal structure of these pellets were analyzed by X-ray diffractometry (XRD).

Table 1
Characteristics of three kinds of Li_2TiO_3 pellets

Items	Specimens		
	Sample A	Sample B	Sample C
Dimension (mm)	8.0 diameter × 2.0 thickness		
Density (%T.D.)	73.3	83.2	92.8
Porosity (%)	26.7	16.8	7.2
Pore radius (μm)	0.30	0.30	0.05
Grain size (μm)	2.4	4.3	25
Specific surface (m^2/g)	0.25	0.13	0.08

Theoretical density of β-$Li_2TiO_3 = 3.43$ g/cm^3.

Specific heat of Li_2TiO_3 powder was measured by differential scanning calorimetry (DSC). Li_2TiO_3 powder, which was 1 μm in grain size, was used for the measurement. The measurement of specific heat was performed at temperatures from room temperature to 1073 K in air. Thermal diffusivity of the three kinds of Li_2TiO_3 pellets

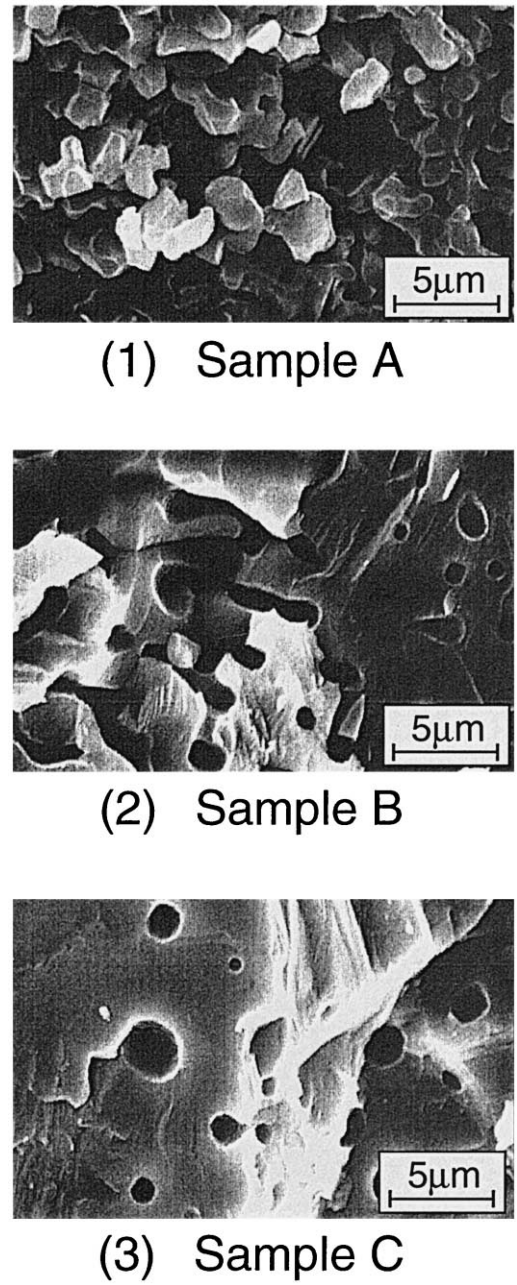

Fig. 2. SEM photographs of cross-sections on each Li_2TiO_3 pellet.

was measured by laser flash method. The environmental pressure was less than 2×10^{-4} Pa. Thermal diffusivity of these pellets was obtained by measuring the temperature elevation on the near surface of the pellets using an infrared temperature sensor and a thermocouple. Thermal conductivity was calculated from these measurement values and from the density of these pellets. Thermal expansion of these Li_2TiO_3 pellets was measured by laser interferometry method. The measurements were performed under a pressure less than 1.3×10^{-4} Pa. The measurements were performed at temperatures from room temperature to 973 K. Thermal hysteresis effects were also examined on each Li_2TiO_3 pellet and was determined by measuring thermal conductivity and thermal expansion five times by laser flash and laser interferometry.

3. Results and discussion

3.1. Material characteristics

The results of density, porosity, specific surface area, and average grain size of the three kinds of Li_2TiO_3 pellets are shown in Table 1. Here, the density calculated by volume and weight of each pellet agreed with the density measured by mercury porosimetry within an error of 4%. Specific surface area decreased with increasing density. SEM photographs of the cross-section of the three kinds of Li_2TiO_3 pellets are shown in Fig. 2. The grain sizes of the Li_2TiO_3 pellets, namely Sample A, Sample B and Sample C were 2.4, 4.3 and 25 μm, respectively (see Table 1). The main impurities (in ppm) of Li_2TiO_3 pellets were as follows: Na, 25; Al, 14; Ca, 5; Zr, < 5; Mg, < 5; Co, < 0.5; Si, 30; Fe, 21; Mn, < 5. The XRD pattern of a Li_2TiO_3 pellet (Sample C) after sintering is shown in Fig. 3. All of the diffraction peaks that are assigned to β-Li_2TiO_3 appeared in the Li_2TiO_3. Therefore, the basic properties of each Li_2TiO_3 pellet, such as density, grain size, specific surface area, chemical composition, etc., were measured for the evaluation of thermal properties.

3.2. Thermal properties

3.2.1. Specific heat

Temperature dependence on specific heat, C_p, of Li_2TiO_3 powder is shown in Fig. 4. These experimental data agreed with the values measured by Christensen et al. [13]. From the results, the specific heat of Li_2TiO_3 is given as follows:

$$C_p(\mathrm{J/g/K}) = 0.73 + 8.44 \times 10^{-4} T/\mathrm{K} - 1.67 \times 10^{-7} T/\mathrm{K}^{-2} \quad (T = 350\text{–}1050\ \mathrm{K}). \tag{1}$$

The specific heat for each Li_2TiO_3 pellet was measured by the laser flash method, however these values were very widely scattered, and were not used in this report here.

3.2.2. Thermal diffusivity

Thermal diffusivity, α, was obtained by the laser flash method. Temperature dependence on thermal diffusivity of Li_2TiO_3 pellets is shown in Fig. 5. From the results, the thermal diffusivity of each Li_2TiO_3 pellet was about 0.9–1.0×10^{-6} m^2/s at room temperature, falling to about 5.0–5.5×10^{-7} m^2/s at the highest measurement temperature. In particular the thermal diffusivity of Sample B, which is 83%T.D., approximately agreed with the data obtained by Davis and Haasz [14].

3.2.3. Thermal conductivity

The values of thermal conductivity are calculated using the following relation:

$$k = \alpha C_p \rho, \tag{2}$$

where k is thermal conductivity in W/m/K, and ρ is the density in g/m^3.

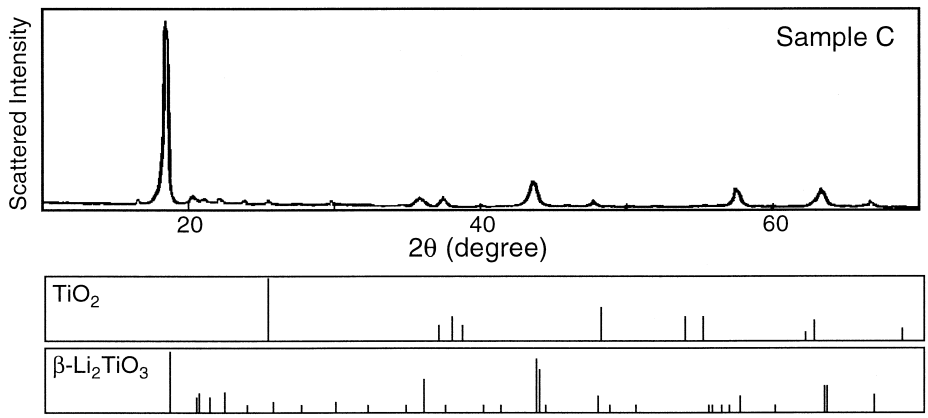

Fig. 3. X-ray diffraction patterns of Li_2TiO_3 pellet (Sample C).

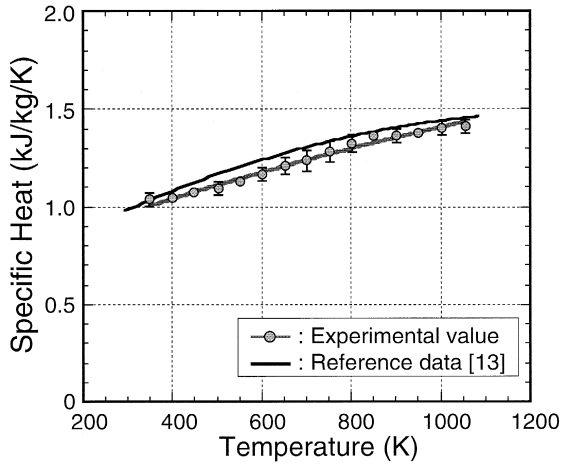

Fig. 4. Temperature dependence of specific heat for Li_2TiO_3 powder as measured by DSC.

Thermal conductivity of a porous material varies not only with the porosity, but also with the grain size and pore shape, the pore distribution, the cracks and so on. These variables may be affected by starting material, preparation procedure, and temperature history of the specimen. There is an equation in common use describing the influence of porosity on the thermal conductivity, the modified Maxwel–Eucken equation, which is as follows [15,16]:

$$k = k_0 \frac{(1-p)}{(1+\beta p)}, \tag{3}$$

where k_0 (W/m/K) is the thermal conductivity when the density is 100%T.D., p is porosity in non-dimensional units, and β is an empirical parameter.

Porosity dependence on thermal conductivity of Li_2TiO_3 pellets is shown in Fig. 6. From this figure, thermal

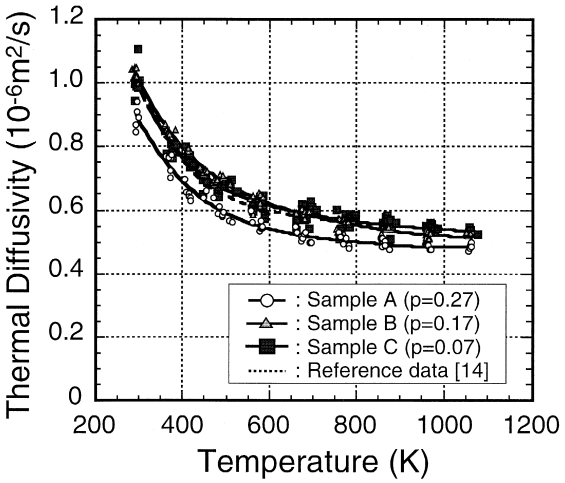

Fig. 5. Temperature dependence of thermal diffusivity for Li_2TiO_3 pellets.

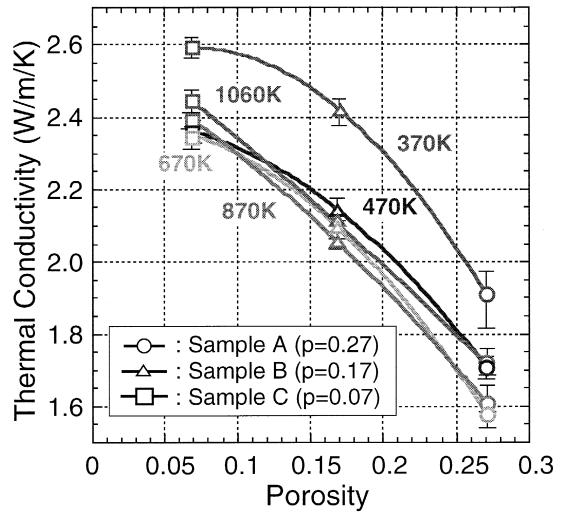

Fig. 6. Porosity dependence of thermal conductivity for Li_2TiO_3 pellets.

conductivity of Li_2TiO_3 pellets at the lower temperatures cannot be fit by a straight line. On the other hand, the thermal conductivity at the higher temperatures was fit by a straight line. The measured data were fitted with Eq. (3), and k_0 and β were calculated. The empirical equation obtained here is as follows:

$$k/\mathrm{W\,m^{-1}\,K^{-1}} = \frac{(1-p)}{(1+\beta p)}\left(4.77 - 5.11\times 10^{-3} T/\mathrm{K} + 3.12\times 10^{-6} T/\mathrm{K}^2\right),$$

$$\beta = 1.06\text{–}2.88\times 10^{-4} T \times (\,p = 0.07\text{–}0.27,\ \rho = 73\text{–}93\%\text{T.D.},\ T = 300\text{–}1050\ \mathrm{K}). \tag{4}$$

Temperature dependence on thermal conductivity of Li_2TiO_3 pellets is shown in Fig. 7. In Fig. 7, thermal

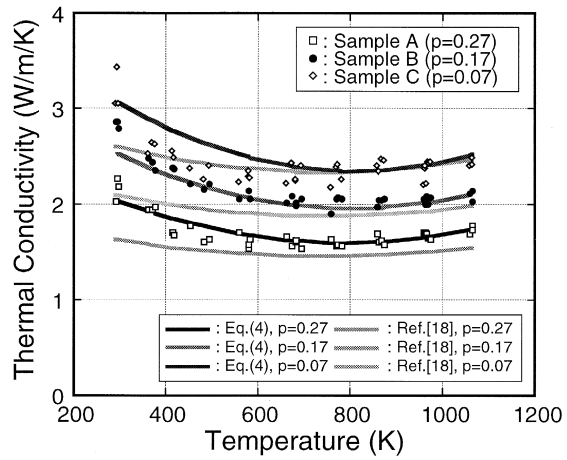

Fig. 7. Temperature dependence of thermal conductivity for Li_2TiO_3 pellets.

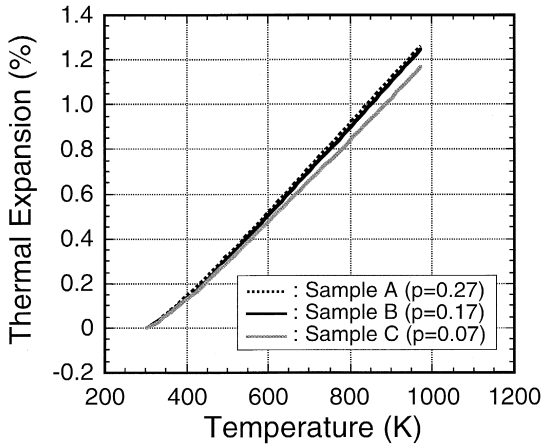

Fig. 8. Temperature dependence of thermal expansion for Li_2TiO_3 pellets.

conductivity values of Samples A and B approximately agree with the values calculated by Eq. (4). Thermal conductivity values of Sample C were lower than the values calculated by Eq. (4). From these results, the values calculated by Eq. (4) can reproduce the experimental data within an error of $\pm 10\%$. Fig. 7 also shows the calculated values of the reference equation, which was reported by Gierszewski et al. [17,18], presented by the dotted line in comparison. Thermal conductivity calculated by Eq. (4) approximately agreed with the reference data at high temperature (> 500 K). However, thermal conductivity calculated by Eq. (4) was higher than that of the reference data at low temperature (< 500 K).

A direct dependence of thermal conductivity on related grain size and pore size is expected because the mean free path of phonon scattering is less than the grain size of Li_2TiO_3 pellets. The pore shape of each Li_2TiO_3 pellet was spherical from the results of SEM observation (see Fig. 2), but the thermal conductivity may be dependent on the pore shape. The variables affecting thermal conductivity may be affected by temperature history of the prepared Li_2TiO_3 pellets.

No thermal hysteresis of Samples A and B was observed in the thermal diffusivity measurements. However, thermal hysteresis of Sample C was observed in the heat-

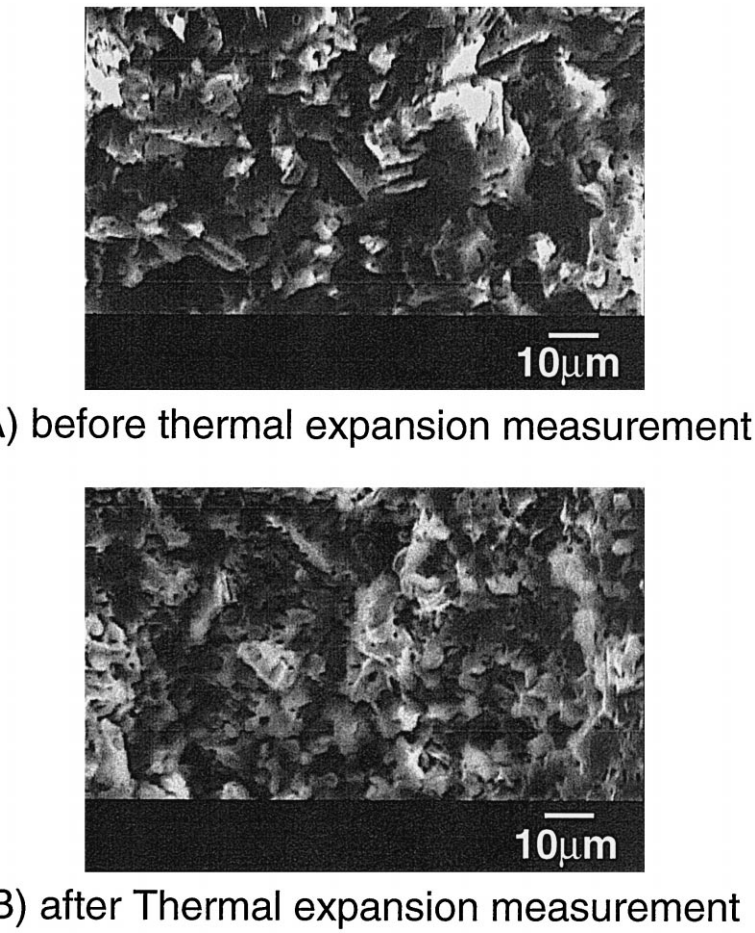

Fig. 9. SEM photographs of Li_2TiO_3 pellet (Sample B) before/after thermal expansion measurement.

ing and cooling cycles. From these results, the thermal hysteresis of Sample C may be affected by temperature history in the pellet preparation. The crystal structure of Li_2TiO_3 changes above 1423 K from β-phase to γ-phase. The crystal structures of β-phase and γ-phase are monoclinic system and cubic system, respectively. Sample C was sintered at 1673 K in the preparation and the grain size of Sample C was large (25 μm). Thus, some cracks may be introduced at grain boundaries in the preparation because of anisotropy in expansion or shrinkage of Li_2TiO_3 matrix.

3.2.4. Thermal expansion

Temperature dependence on thermal expansion of Li_2TiO_3 pellets is shown in Fig. 8. Thermal expansion of Sample A approximately agreed with that of Sample B. However, thermal expansion of Sample C was smaller than those of Samples A and B. It seems that Sample C contains internal cracks from the preparation. Therefore, the thermal expansion of Li_2TiO_3 was calculated using the measured value of Sample A and B and is given as follows.

$$L = -0.578 + 1.71 \times 10^{-3} T/\mathrm{K} + 1.867 \times 10^{-7} T/\mathrm{K}^2 \times (T = 373\text{–}1073\ \mathrm{K},\ p = 0.26\text{–}0.15 \times (\rho = 73\text{–}85\%\mathrm{T.D.})). \quad (5)$$

Thermal expansion of Li_2TiO_3 pellets approximately agreed with the measured value of a thin Li_2TiO_3 specimen, which was reported by Girard et al. [19]. SEM photographs of fracture cross section of Li_2TiO_3 pellet (Sample B) before/after thermal expansion measurement are shown in Fig. 9. Microstructure of Sample B did not change after 7 thermal expansion measurements. On the other hand, the thermal expansion of Sample C was smaller than that of these pellets (Sample A and B). Small cracks may exist in Sample C.

Thermal hysteresis of each Li_2TiO_3 pellet was not observed during heating and cooling cycles in thermal expansion experiments and Li_2TiO_3 appears to be stable during temperature cycling between room temperature and 1100 K.

4. Conclusion

As a part of the research program for fusion blanket development, characterization of Li_2TiO_3 pellets has been performed for the material selection and fusion blanket design. The basic properties of each Li_2TiO_3 pellet, such as density, grain size, specific surface area chemical composition, etc., were measured for the evaluation of thermal properties. The thermal properties, such as specific heat, thermal diffusivity and thermal expansion of the three kinds of Li_2TiO_3 pellets, were measured up to 1100 K. Density dependence on thermal conductivity was expressed by the modified Maxwel–Eucken equation. Thermal hysteresis of Li_2TiO_3 was not observed during heating and cooling cycles in thermal diffusivity and thermal expansion measurements. Li_2TiO_3 appears to be stable to temperatures between room temperature and 1100 K.

Acknowledgements

We greatly appreciate the helpful comments on this paper by Dr O. Baba (Director, Department of JMTR, JAERI).

References

[1] C.E. Johnson, K.R. Kummerer, E. Roth, J. Nucl. Mater. 155–157 (1988) 188.
[2] C.E. Johnson, J. Nucl. Mater. 179–181 (1991) 42.
[3] M.S. Ortman, E.M. Larsen, J. Am. Soc. 66 (1983) 645.
[4] C. Alvani, S. Casadio, L. Lorenzini, G. Brambilla, Fusion Technol. 10 (1986) 106.
[5] J.W. Kammeyer, O.J. Whittemore, Adv. Ceram. 25 (1989) 117.
[6] H. Hamilton, J. Nucl. Mater. 219 (1996) 274.
[7] D. Vollath, H. Wedemeyer, Adv. Ceram. 25 (1989) 93.
[8] D.L. Smith, J. Nucl. Mater. 122&123 (1984) 51.
[9] P. Groner, W. Scifritz, Nucl. Technol./Fusion 5 (1984) 169.
[10] N. Roux, J. Avon, A. Floreancig, J. Mougin, B.R. Asneur, S. Ravel, in: Proc. 4th Int. Workshop on Ceramic Breeder Blanket Interactions, 1995, p. 452.
[11] K. Tsuchiya, H. Kawamura, M. Saito, K. Tatenuma, M. Kainose, J. Nucl. Mater. 219 (1996) 246.
[12] K. Tsuchiya, H. Kawamura, T. Takeuchi, ISFNT-4 (to be published).
[13] A. Christensen, K.C. Conway, K.K. Kelley, US Bur. Mines Report RI-5565, 1960.
[14] J.W. Davis, A.A. Haasz, J. Nucl. Mater. 232 (1996) 65.
[15] G. Ondracek, B. Schulz, J. Nucl. Mater. 46 (1973) 253.
[16] Y. Takahashi, T. Terai, T. Ohsato, H. Kawamura, Adv. Ceram. 27 (1989) 199.
[17] P. Finn, T. Kurasawa, N. Nau, K. Noda, H. Watanabe, in: Proc. IEEE 9th Symp. on Engineering Problems of Fusion Research, vol. II, 1981, p. 1200.
[18] P. Gierszewski, CFFTP G-9596, 1995.
[19] D.T. Girard, C.T. Sims, H.R. Wisely, US Patent 3,397,080, 1960.